

Temperature and doping dependence of the penetration depth in $\text{Bi}_2\text{Sr}_2\text{CaCu}_2\text{O}_{8+\delta}$

O. Waldmann,* F. Steinmeyer,† and P. Müller*

Walther-Meißner-Institut, Walther-Meißner-Strasse 8, D-85748 Garching, Germany

J. J. Neumeier

Los Alamos National Laboratory, Los Alamos, New Mexico 87545

F. X. Régi, H. Savary, and J. Schneck

France Télécom, Centre National d'Etudes des Télécommunications de Bagneux, F-92220 Bagneux, France

(Received 8 December 1995)

Using torque magnetometry in the Shubnikov state, we have studied the London penetration depth $\lambda_{ab}(T)$ of $\text{Bi}_2\text{Sr}_2\text{CaCu}_2\text{O}_{8+\delta}$ and $(\text{Pb}_x\text{Bi}_{1-x})_2\text{Sr}_2\text{CaCu}_2\text{O}_{8+\delta}$ single crystals with different oxygen excess δ . With increasing charge carrier density $n_s/m^* \propto 1/\lambda_{ab}^2(0)$ the transition temperature at first increases, then approaches a maximum, and finally decreases. The sample independent, universal behavior found in the 1:2:3 family is not confirmed. Dependent on preparation prehistory of the samples, either linear or quadratic low temperature behavior of $\lambda_{ab}(T)$ was observed. A linear term is seen for samples with high maximum $T_c \approx 94$ K, while samples with quadratic behavior show a significantly reduced T_c . The results are discussed in terms of d -wave superconductivity with resonant impurity scattering.

In the current debate on possible pairing mechanisms in high temperature superconductors, penetration depth measurements can provide two important contributions.

(1) The transition temperature T_c is highly sensitive to the ratio of the Cooper pair density n_s to the electron effective mass m^* [$n_s/m^* \propto 1/\lambda_{ab}^2(0)$]. m^* is the electron effective mass for transport parallel to the CuO_2 layers. Previous investigations yielded conflicting results. In muon spin-relaxation (μSR) measurements in a wide class of high temperature superconductors (HTSC's), Uemura *et al.*¹ reported a universal linear relation between T_c and n_s/m^* at low carrier doping levels, whereas in heavily doped samples saturation or a slight decrease was observed. In contrast, in μSR measurements in $\text{Bi}_{2-x}\text{Pb}_x\text{Sr}_2\text{Ca}_{1-z}\text{Y}_z\text{Cu}_2\text{O}_{8+\delta}$ with different x , z , and δ , Weber *et al.*² found no systematic T_c vs n_s/m^* correlation, although n_s/m^* varied by a factor of almost 2. In a magnetization study of samples with different oxygen content, Däumling *et al.*³ found a variation of the transition temperatures while the absolute values of the penetration depth remained unchanged.

(2) The penetration depth at low temperatures allows different classes of pairing mechanisms to be separated. A superconductor with s -wave pairing exhibits a finite excitation energy with a minimum energy gap Δ_{\min} . Therefore for clean superconductors $\lambda(T)$ at low temperatures varies as $\lambda(T) - \lambda(0) \propto \exp(-\Delta_{\min}/k_B T)$. In contrast, all of the possible non- s -wave spin singlet pairing states of a superconductor with tetragonal or orthorhombic symmetry and a spherical or cylindrical Fermi surface have line nodes in the gap leading to a linear temperature dependence,^{5,6} $\lambda(T) - \lambda(0) \propto T$, in the clean limit. Impurity scattering changes the temperature dependence of the penetration depth for both s - and d -wave models.⁷ For sufficiently strong scattering a quadratic temperature dependence, $\lambda(T) - \lambda(0) \propto T^2$, is obtained.⁷ In the standard Born approximation, a

high impurity concentration would be required to obtain a quadratic law, resulting in a strong decrease of T_c which has not been observed.⁷ However, for a d -wave superconductor with resonant scattering even a small impurity concentration n_i gives rise to a quadratic temperature dependence below a crossover temperature⁸ $T^* \propto \sqrt{n_i}$. Above T^* the linear term is conserved. The small impurity concentration n_i decreases T_c only slightly. Recently, in a series of experiments on $\text{YBa}_2\text{Cu}_3\text{O}_7$ (YBCO) single crystals and epitaxial YBCO films, a linear temperature dependence has been measured at low temperatures,⁹ in contrast to the quadratic behavior observed earlier.¹⁰ After adding a small concentration of zinc impurities, the linear temperature dependence was shown to change to quadratic behavior below a crossover temperature.¹¹ On the other hand, in YBCO films an exponential temperature dependence has also been reported.¹² In the case of $\text{Bi}_2\text{Sr}_2\text{CaCu}_2\text{O}_8$ (BSCCO) quadratic temperature dependencies have been observed so far.^{10,13}

Compared to YBCO, BSCCO is a simpler HTSC system; there are no CuO chains which can mask any clear doping dependence. Furthermore, it is extremely anisotropic,¹⁴ nearly two dimensional,¹⁵ and has only a small orthorhombic distortion from the tetragonal unit cell.¹⁶ The aim of this work is to investigate the temperature and oxygen doping dependence of the penetration depth in BSCCO in more detail. In the following we first develop the method used to measure $\lambda_{ab}(T)$. Then setup and sample preparation are described. After the method's experimental check the results are discussed. We close with a conclusion.

Our experimental approach allows the measurement of the temperature dependence of the penetration depth for magnetic fields perpendicular to the CuO_2 planes, $\lambda_{ab}(T)$, with high resolution as well as the precise determination of its absolute value. As has been shown earlier, for intermediate external fields, $H_{c1} \ll H \ll H_{c2}$, the penetration depth can be determined from the reversible magnetization contributed

by the closely packed arrangement of vortices.¹⁷ In the anisotropic Ginzburg-Landau model of Hao and Clem,¹⁸ the magnetization perpendicular to the CuO₂ planes is given by

$$M_{\perp} = -\frac{\alpha\Phi_0}{8\pi\mu_0\lambda_{ab}^2} \ln \frac{\beta H_{c2\perp}}{H \cos\Theta} \quad (1)$$

where Θ is the angle between the magnetic field and c axis of the sample, and $\alpha=0.77$, $\beta=1.44$ are constants in the field range $0.02 < H/H_{c2\perp} < 0.3$. Φ_0 is the magnetic flux quantum and $\mu_0 = 4\pi \times 10^{-7}$ V s/A m. Because of the large magnetic anisotropy $\gamma = \lambda_c/\lambda_{ab}$ of BSCCO [$\gamma = 240\text{--}900$ (Ref. 14)] the magnetic properties can be regarded as two dimensional in a wide angle range¹⁹ $\tan\Theta < \gamma$ (e.g., $\tan 89.8^\circ = 240$). The component of magnetization parallel to the CuO₂ planes, M_{\parallel} , is smaller than M_{\perp} by an order of γ . Therefore, the magnetization being normal to the planes with high accuracy, the resulting torque is

$$\tau = -\mu_0 V M_{\perp} H \sin\Theta \quad (2)$$

where V is the volume of the sample. Instead of evaluating $dM_{\perp}/d \ln H \propto \Phi_0/\lambda_{ab}^2$ [Eq. (1)] at fixed temperature points, we can enhance the resolution of the measurement of the temperature dependence of the penetration depth by applying a temperature sweep method in a fixed field. If $\beta H_{c2\perp}(T)$ is known with logarithmic accuracy, both the temperature dependence and the absolute value of $\lambda_{ab}(T)$ can be determined from torque $\tau(T, H = \text{const})$. As the superconducting volume may be smaller than the sample volume, the determined values of the penetration depth are upper bounds. The following points confirm that the method is highly reliable in BSCCO.

(1) Due to the short coherence lengths $\xi \ll \lambda$ in HTSC's, local theories are an excellent approximation.^{17,3} Furthermore, in BSCCO with Ginzburg-Landau parameter $\kappa \approx 130$, $H_{c1} \ll H \ll H_{c2}$ is a wide field range experimentally.

(2) The reversible magnetization is insensitive to geometric properties of the vortex lattice. In the simple London theory the parameter β in Eq. (1) describes the specific vortex lattice configuration²⁰ (hexagonal, square, amorphous, liquid, etc.), but depends only weakly on it. This is analogous to the small dependence of the Abrikosov parameter β_A on vortex structure (hexagonal: $\beta_A = 1.16$, square: $\beta_A = 1.18$).²⁰ In the treatment of Hao and Clem based on the more precise Ginzburg-Landau model, the small energy differences between specific vortex structures are even neglected.¹⁸ The parameter β (and α) now describes the corrections to the London model due to contributions from the core condensation energy and kinetic energy associated with gradients in the magnitude of the order parameter.

(3) Many alternative methods widely used to measure the penetration depth are based upon the spatial dependence of the magnetic field. For example, microwave techniques determine the penetration depth from the spatial field dependence $B = B(\vec{r}/\lambda)$ at a surface in the Meissner state;²⁰ μ SR techniques measure the weak magnetic field distribution $\langle \Delta B^2 \rangle \propto \lambda^{-4}$ between vortices in the mixed state.²¹ However, in the method presented here the penetration depth is determined essentially by the value of the magnetization M_{\perp}

$\propto \Phi_0/\lambda_{ab}^2$ induced by superconducting currents, averaged over the bulk of the sample. This eliminates possible sources of errors such as shape effects, thermal expansion of the sample, surface effects, fissures, surface degradation (O₂ deficiency), multiply connected material, etc. Furthermore, in fields of about 10 T the magnetization is about a thousand times smaller than the field [$M_{\perp}(H=10 \text{ T}) \sim 10 \text{ mT}$]. Therefore demagnetization effects can clearly be neglected.

(4) In conventional type II superconductors it is hard to achieve a reversible magnetization. However, in HTSC's and especially in BSCCO, the small pinning gives access to the reversible magnetization over a wide temperature and field range. Compared to conventional methods for determining the irreversibility line, e.g., ac susceptibility or evaluation of magnetization curves $M(H, T = \text{const})$, the presented method working in a strict dc-field mode yields a low lying irreversibility line.

(5) The method's range of validity can be determined experimentally. As long as reversibility, scaling, and $M_{\perp} \propto \ln(H)$ are fulfilled simultaneously, any other known contribution to the magnetization is negligible (e.g., fluctuations). Scaling will be explained below.

(6) In the quasi-two-dimensional (2D) regime, $\tan\Theta < \gamma$, the layered structure of the superconductor and any details of the weak interlayer coupling are unimportant. For instance, the 2D limit of the anisotropic London or Ginzburg-Landau theory is equivalent to that of the Lawrence-Doniach model.¹⁹

The torque was measured with a torsion wire magnetometer¹⁴ (diameter 26 mm, length 30 mm) which provides a high resolution of $\Delta\tau = 10^{-12}$ Nm. This allows the temperature dependence of the penetration depth to be determined with a resolution of 1 Å for typical sample weights of 100 μg and fields up to 16 T. A small and reproducible thermal drift amounts to about 10% of the signal between 4 K and 120 K and has been subtracted in each case. The uncertainty of the absolute value (~ 2000 Å) is estimated as ± 100 Å and is composed of the following three contributions. Torques are calibrated to within 3% accuracy by a small coil next to the sample, the orientation of the sample relative to the field can be determined with a precision of 0.9°, and finally the sample volume was calculated from the mass using a density of 6.6 g/cm⁻³ with an error < 1%. For the temperature measurements a Cernox[®] sensor (Lake Shore Cryotronic, Inc.) calibrated with an accuracy of 8 mK was used. The sensor's magnetoresistance in fields up to 16 T leads to a maximum temperature error of 0.5% at 4.2 K, which decreases rapidly with increasing temperature and therefore can be neglected. Transition temperatures of the samples were determined from the onset of the superconducting magnetization with an accuracy of 0.5 K in good agreement with resistive methods.

BSCCO single crystals were grown by a self-flux method in alumina (batches I and II) or gold crucibles (batches III and IV). Details of preparation have been described elsewhere.^{14,22} The single-crystal structure was confirmed using x-ray diffraction. The stoichiometries of all the samples were determined by x-ray microprobe fluorescence (values given in Table I). Variations in samples from the same batch were small (3 at %). The oxygen content was varied by annealing the samples in flowing argon or oxygen at ambient

TABLE I. Stoichiometry of the batches as measured by microprobe analysis.

Batch	Lead content	Stoichiometry
I	12% Pb	$\text{Pb}_{0.26}\text{Bi}_{1.74}\text{Sr}_{1.85}\text{Ca}_{0.9}\text{Cu}_{1.95}\text{O}_{8+\delta}$
II	20% Pb	$\text{Pb}_{0.38}\text{Bi}_{1.75}\text{Sr}_{1.75}\text{Ca}_{1.1}\text{Cu}_{2.0}\text{O}_{8+\delta}$
III	Pb free	$\text{Bi}_{2.1}\text{Sr}_{1.9}\text{Ca}_{0.74}\text{Cu}_{2.0}\text{O}_{8+\delta}$
IV	Pb free	$\text{Bi}_{2.1}\text{Sr}_{1.7}\text{Ca}_{1.1}\text{Cu}_{2.0}\text{O}_{8+\delta}$

pressure and at temperatures between 550 °C and 650 °C. Due to the small diffusion constants in BSCCO,²³ annealing times ranged between 4 and 8 days. Samples B, C, and D were annealed several times in different atmospheres, and sample A was annealed in oxygen atmosphere under high pressure (300 bar) at 440 °C. Because of the small sample size, the precise oxygen content could not be determined, for example, by iodometric titration.

Figure 1 shows that the data are in excellent agreement with the relation $M_{\perp}(H) \propto \ln(H)$ in the field range between 5 T and 16 T. The extrapolation to $\mu_0 M_{\perp} = 0$ T yields $\ln[\beta\mu_0 H_{c2\perp}] = \ln[150 \pm 20 \text{ T}]$ independent of temperature up to $T \sim 0.85T_c$. As was observed by Cho *et al.*,²⁴ the magnetization obeys a scaling law $M_{\perp}(T, H) = f(T)g(H)$ over a wide temperature range. Equation (1) then implies that $\beta H_{c2\perp}$ is temperature independent. The factorization of the magnetization into a temperature independent term and a field independent term can be seen in Figs. 1 and 2, respectively. The deviations from this scaling behavior above $\sim 0.85T_c$ (see Fig. 2) can be explained by the temperature dependence of $\beta H_{c2\perp}$ and by thermal vortex fluctuations.²⁵ From measurements of the quasiparticle scattering intensity in the Raman effect²⁶ and the temperature dependence of the Josephson critical current²⁷ a very weak temperature dependence for the energy gap is seen for Ar-annealed samples from batch III (see Table II), while O₂-annealed samples ap-

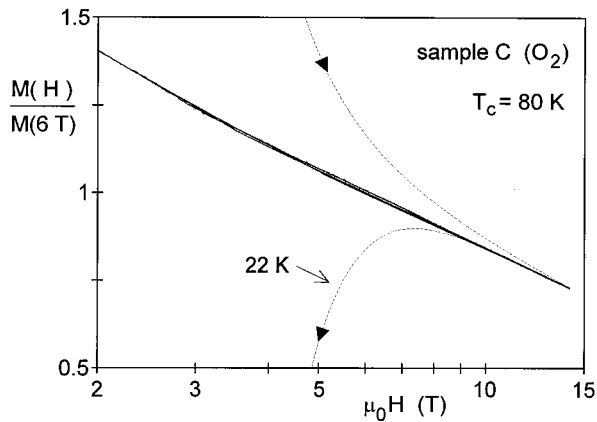


FIG. 1. Magnetization normalized to the value at $\mu_0 H = 6$ T vs $\ln(H)$ at different temperatures. The 22 K curve is strongly hysteretic. The 30 K, 40 K, and 50 K curves lie on the same line. The curves for 60 K and 70 K show only very small deviations from the scaling law. Extrapolating to $\mu_0 M_{\perp} = 0$ T yields $\ln[\beta\mu_0 H_{c2\perp}] = \ln[150 \text{ T}]$ for all curves.

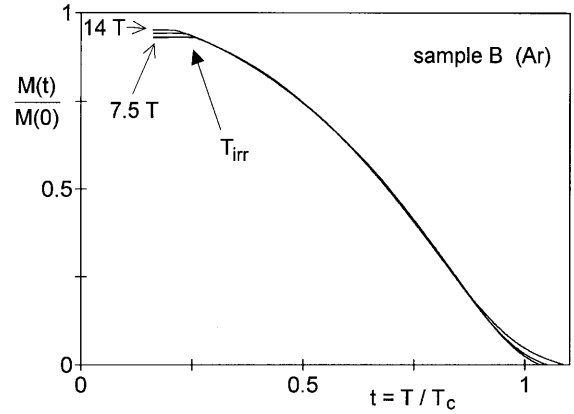


FIG. 2. Magnetization normalized to the extrapolated value at $T = 0$ K vs temperature T . Fields were 7.5 T, 10 T, and 14 T from bottom to top. Towards low temperatures the magnetization freezes as the field dependent irreversibility line is crossed. At temperatures above $\sim 0.85T_c$ the curves spread under the combined influence of thermal vortex fluctuations and a noticeable temperature dependence of $\beta H_{c2\perp}$. In the intermediate temperature range scaling is perfect.

pear to be similar to the BCS behavior. A very weak temperature dependence was also seen for as grown samples.²⁸ The gap is related to the upper critical field via the coherence length by $\mu_0 H_{c2\perp} = \Phi_0 / 2\pi \xi_{ab}^2$ and $\xi_{ab} \approx \hbar v_F / \pi \Delta$ (v_F is the Fermi velocity).^{20,24} A weak temperature dependence even for O₂-annealed samples can be seen in Fig. 1. As the penetration depth is determined from the reversible magnetization, this method is limited to temperatures above the irreversibility line $T_{irr}(H)$. This is indicated by an arrow in Fig. 2. Once the temperature decreases below the irreversibility temperature T_{irr} , the vortices get pinned and the magnetization deviates from its equilibrium value.

Table II lists the most important properties of the investigated samples in different annealing states. $\lambda_{ab}(0)$ was determined by extrapolating the low temperature power law to $T = 0$ K (see below). The small values of $\lambda_{ab}(0)$ and the high maximum T_c indicate excellent sample quality. For every sample, the ratio of the charge carrier density to the effective mass, given in the London theory by $n_s/m^* = [\mu_0 e^2 \lambda_{ab}^2(0)]^{-1}$, increases with growing oxygen doping. The arrows in Fig. 3 indicate the direction of increasing oxygen content. T_c as a function of oxygen content thus possesses the well-known maximum.²⁹ As T_c versus n_s/m^* behaves in the same manner (Fig. 3), n_s/m^* varies roughly proportionally to the oxygen content. It is remarkable that n_s/m^* for the Pb-doped sample B depends only weakly on oxygen doping, although there is a striking influence on T_c . Compared to the Pb-free samples, an increase of n_s/m^* by Pb doping is absent, although Pb should introduce additional holes. It was argued earlier that the Pb-doped holes are immobile and therefore do not contribute to the charge carrier density.² For sample C the T_c maximum is shifted to lower n_s/m^* although its Ca deficiency implies the addition of holes. The universal behavior for T_c versus n_s/m^* found by Uemura *et al.*¹ cannot be confirmed for BSCCO. A proportionality of T_c and n_s/m^* for low doping

TABLE II. Sample characterization. The samples were annealed in the sequence given in the column ‘‘Anneal.’’ The annealing temperature was 550 °C–650 °C. The penetration depth is characterized by the low temperature behavior $\lambda(T)/\lambda(0)=1+\alpha T^\beta$ with $\beta=1$ or $\beta=2$. The accuracy of T_c and $\lambda_{ab}(0)$ are given in the text, that of α is 3%.

Sample	Batch	Mass	Anneal	T_c	$\lambda_{ab}(0)$	$\alpha=\Delta[\lambda/\lambda(0)]/\Delta T^\beta$	β
A	I	108 μg	O ₂ 300 bar	68 K	1900 Å	$15.4\times 10^{-5} \text{ K}^{-2}$	2
B	II	300 μg	as grown	89 K	2200 Å	$9.15\times 10^{-5} \text{ K}^{-2}$	2
			Ar	87 K	2300 Å	$7.24\times 10^{-5} \text{ K}^{-2}$	2
			O ₂	71.5 K	2000 Å	$12.3\times 10^{-5} \text{ K}^{-2}$	2
C	III	87 μg	as grown	88 K	2700 Å	$9.03\times 10^{-5} \text{ K}^{-2}$	2
			O ₂	80 K	2250 Å	$8.42\times 10^{-5} \text{ K}^{-2}$	2
D	IV	190 μg	as grown	94 K	2050 Å	$3.92\times 10^{-3} \text{ K}^{-1}$	1
			Ar	80 K	2700 Å	$3.93\times 10^{-3} \text{ K}^{-1}$	1
			O ₂	85.5 K	1950 Å	$2.86\times 10^{-3} \text{ K}^{-1}$	1

levels and perhaps even for high doping cannot be excluded, but the slopes and offsets are certainly not universal. Even if one stays within the BSCCO family, they vary from batch to batch, i.e., with precise batch stoichiometry. The data of Weber *et al.*² did not exhibit a significant T_c variation to within 10 K. They studied samples differing in the oxygen concentration as well as a second component (e.g., Ca) which both enter n_s/m^* . Thus a T_c maximum as a function of δ might be masked in the T_c vs n_s/m^* diagram. It must be concluded that in view of the complex phase equilibria of BSCCO a comparison of the charge carrier density between different stoichiometries is questionable. Furthermore, a wide range of n_s/m^* is realized in the BSCCO system, which is not due to simple doping arithmetics. We remark that in general m^* defined by $\lambda_{ab}^2 = m^*/\mu_0 e^2 n_s$ is not related to the band effective mass for transport in the CuO₂ layers except in the special cases of a spherical or elliptical Fermi surface and an isotropic gap.³⁰ For HTSC's showing a more complex Fermi surface and potentially anisotropic gap the deduction of m^* is more complex.³⁰

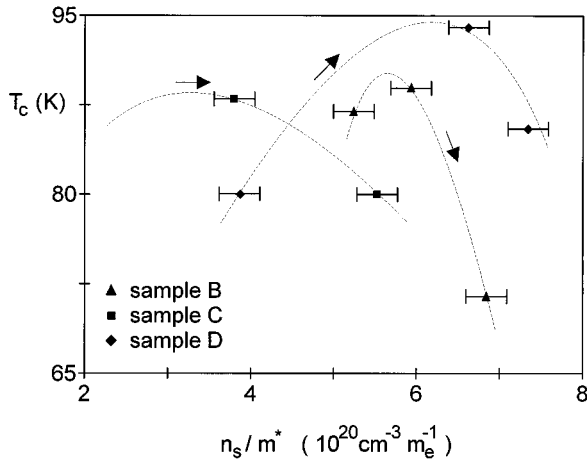


FIG. 3. Transition temperature T_c vs n_s/m^* . The dashed lines interconnect the data of one sample. Arrows indicate the direction of increasing oxygen content.

The temperature dependence of the penetration depth for different samples is shown in Fig. 4. It is striking that all the measured curves lie below those of the BCS theory with isotropic energy gap. $\lambda_{ab}(T)$ depends on the sample batch as well as on the oxygen content. The effect of these two factors is best seen by approximating the penetration depth at low temperatures by a power law $\lambda_{ab}(T)/\lambda_{ab}(0)=1+\alpha T^\beta$ with $\beta=1$ or $\beta=2$ (Fig. 5). The dependence of $\lambda_{ab}(0)$ on batch and oxygen content has been discussed above. The exponent β is independent of the annealing conditions and splits the samples into two groups. First, sample D shows a linear temperature dependence of $\lambda_{ab}(T)$ ($\beta=1$) at all three oxygen doping levels. The slope α decreases with increasing oxygen content and increasing n_s/m^* , respectively. Second, the other samples with parabolic behavior ($\beta=2$) have a T_c maximum lowered by about 5 K. In the Pb-free sample (C) α increases with decreasing n_s/m^* while in the Pb-doped sample (B) α decreases. An interpretation of the be-

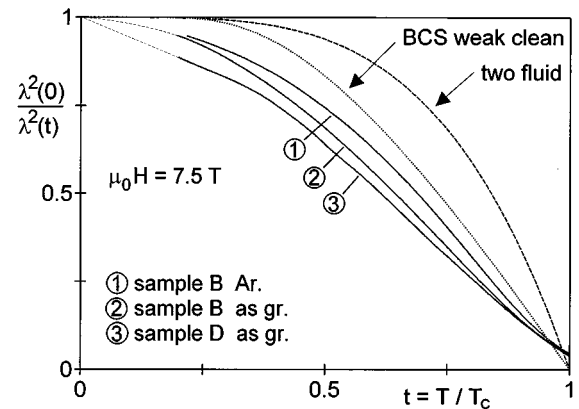


FIG. 4. Temperature dependence of the normalized penetration depth. Sample codes are given from top to bottom in the order of the low temperature values (see Table II). Due to fluctuations the curves do not vanish at T_c (see Fig. 2 and text). For comparison, the two-fluid model and the BCS result for clean superconductors in the weak coupling limit are included.

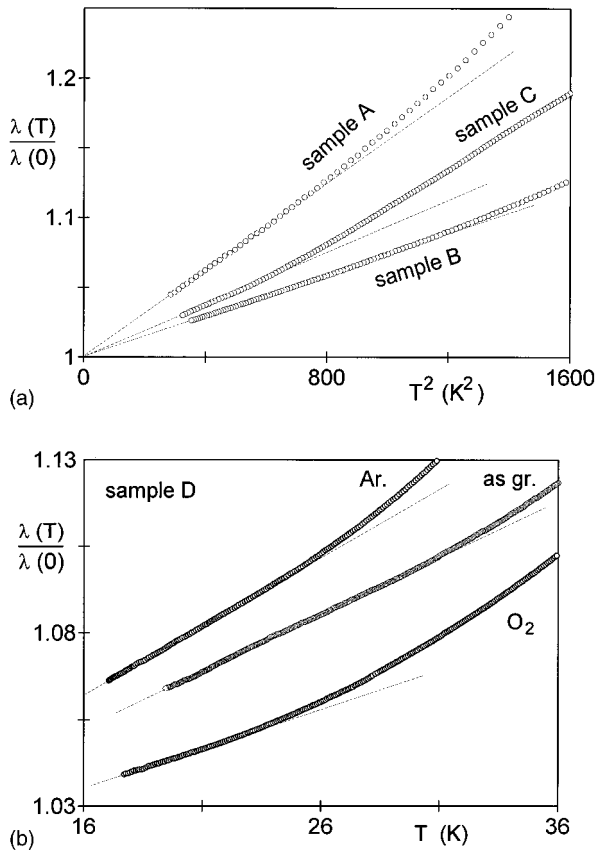


FIG. 5. Penetration depth vs temperature at low temperatures. Samples A, B, and C show a parabolic dependence (a) whereas sample D shows a linear behavior (b).

havior of the slope α is not yet known. The exponent β could be explained in terms of a suppression of T_c due to impurities as given by the Abrikosov-Gorkov³¹ relation, which holds for both s - and d -wave superconductors.⁸

Therefore the large maximum T_c of sample D can be linked to a small impurity concentration and, according to d -wave theory with resonant scattering described above, to a small crossover temperature T^* . As the linear term has been observed in the experimentally accessible range above 17 K, T^* at best is below 17 K. On the other hand, the reduced T_c maxima of the other batches indicate an increased crossover temperature T^* which can explain the observed quadratic temperature dependence of $\lambda_{ab}(T)$. Within this picture it is striking that D, like the others, shows the T_c maximum. This indicates that this maximum indeed is an intrinsic property of the superconducting state and not an artifact of, e.g., impurities introduced by doping. The microscopic origin of the resonant scattering in HTSC's is not yet known, as was pointed out by the authors of Ref. 8.

In conclusion, we have shown that for the highly anisotropic superconductor $\text{Bi}_2\text{Sr}_2\text{CaCu}_2\text{O}_{8+\delta}$ the penetration depth $\lambda_{ab}(T)$ can be determined from the reversible magnetization. High sensitivity torque magnetometry allows the measurement of both the temperature dependence of $\lambda_{ab}(T)$ with high resolution and its absolute value with high accuracy. Because T_c and the penetration depth depend sensitively on the cation and oxygen stoichiometry, the comparison of experimental data requires care. A linear temperature dependence of $\lambda_{ab}(T)$ at low temperatures is observed in conjunction with a high maximum T_c . It is noticeable that the linear temperature dependence remains unchanged upon oxygen doping. Samples with significantly reduced T_c show a quadratic temperature dependence. These results are consistent with a $d_{x^2-y^2}$ -wave model with resonant impurity scattering.

The authors wish to thank D. Einzel, G. Hechtfischer, C. Reimann, B. Schey, K. Schlenga, and W. Walkenhorst for valuable discussions. Partial financial support by the Bayerische Forschungstiftung via the FORSUPRA consortium is gratefully acknowledged.

*Present address: Physikalisches Institut III der Universität Erlangen, Erwin-Rommel-Strasse 1, D-91058 Erlangen, Germany.
 †Present address: Siemens AG (Corporate Research) ZFE T EP 4, Box 3220, D-91058 Erlangen, Germany.
¹Y. J. Uemura *et al.*, Phys. Rev. Lett. **62**, 2317 (1989); **66**, 2665 (1991).
²M. Weber *et al.*, Phys. Rev. B **48**, 13 022 (1993).
³M. Däumling and G. V. Chandrasekhar, Phys. Rev. B **46**, 6422 (1992).
⁴B. Mühlischlegel, Z. Phys. **155**, 313 (1959).
⁵J. Annett, N. Goldenfeld, and S. R. Renn, Phys. Rev. B **43**, 2778 (1991).
⁶F. Gross, B. S. Chandrasekhar, D. Einzel, K. Andres, P. J. Hirschfeld, H. R. Ott, J. Beuers, Z. Fisk, and J. L. Smith, Z. Phys. B **64**, 175 (1986).
⁷P. Arberg, M. Mansor, and J. P. Carbotte, Solid State Commun. **86**, 671 (1993).
⁸P. J. Hirschfeld and N. Goldenfeld, Phys. Rev. B **48**, 4219 (1993).
⁹O. M. Froehlich, H. Schulze, R. Gross, A. Beck, and L. Alff, Phys. Rev. B **50**, 13 894 (1994); J. E. Sonier *et al.*, Phys. Rev. Lett. **72**, 744 (1994); W. N. Hardy, D. A. Bonn, D. C. Morgan, R. Liang, and K. Zhang, *ibid.* **70**, 3999 (1993).

¹⁰M. R. Beasley, Physica C **209**, 43 (1993); Z. Ma *et al.*, Phys. Rev. Lett. **93**, 781 (1993).
¹¹D. Achkir, M. Poirier, D. A. Bonn, R. Liang, and W. N. Hardy, Phys. Rev. B **48**, 13 184 (1993).
¹²S. M. Anlage *et al.*, Phys. Rev. B **44**, 9764 (1991); N. Klein *et al.*, Phys. Rev. Lett. **71**, 3355 (1993).
¹³A. Maeda, T. Shibauchi, N. Kondo, K. Uchinokura, and M. Kobayashi, Phys. Rev. B **46**, 14 234 (1992).
¹⁴F. Steinmeyer, R. Kleiner, P. Müller, H. Müller, and K. Winzer, Europhys. Lett. **25**, 459 (1994).
¹⁵P. H. Kes *et al.*, Phys. Rev. Lett. **67**, 2383 (1991).
¹⁶W. E. Pickett, Rev. Mod. Phys. **61**, 433 (1989); A. I. Beskrovnyi *et al.*, Physica C **166**, 79 (1990).
¹⁷V. G. Kogan, M. M. Fang, and S. Mitra, Phys. Rev. B **38**, 11 958 (1988).
¹⁸Z. Hao and J. R. Clem, Phys. Rev. Lett. **67**, 2371 (1991).
¹⁹D. Feinberg, Physica C **194**, 126 (1992).
²⁰M. Tinkham, *Introduction to Superconductivity* (McGraw-Hill, New York, 1975).
²¹B. Pümpin *et al.*, Phys. Rev. B **42**, 8019 (1990).
²²F. X. Régi, J. Schneck, H. Savary, C. Daguët, and F. Huet, IEEE Trans. Appl. Supercond. **1**, 1190 (1993).

- ²³M. Runde *et al.*, Phys. Rev. B **45**, 7375 (1992).
- ²⁴J. H. Cho, Z. Hao, and D. C. Johnston, Phys. Rev. B **46**, 8679 (1992).
- ²⁵V. G. Kogan, M. Ledvij, A. Y. Simonov, J. H. Cho, and D. C. Johnston, Phys. Rev. Lett. **70**, 1870 (1993).
- ²⁶T. Stauffer, R. Nemetschek, R. Hackl, P. Müller, and H. Veith, Phys. Rev. Lett. **68**, 1069 (1992).
- ²⁷R. Kleiner, F. Steinmeyer, G. Kunkel, and P. Müller, Phys. Rev. Lett. **68**, 2394 (1992).
- ²⁸M. Boekholt, M. Hoffmann, and G. Güntherodt, Physica C **175**, 127 (1991).
- ²⁹C. Allgeier and J. S. Schilling, Physica C **168**, 499 (1990); W. A. Groen, D. M. de Leeuw, and L. F. Feiner, *ibid.* **165**, 55 (1990).
- ³⁰B. S. Chandrasekhar and D. Einzel, Ann. Phys. (Leipzig) **2**, 535 (1993).
- ³¹A. A. Abrikosov and L. P. Gor'kov, Zh. Éksp. Teor. Fiz. **39**, 1781 (1960) [Sov. Phys. JETP **12**, 1243 (1960)].